

Time-Resolved Mass Spectrometry of the Exothermic Reaction between Nanoaluminum and Metal Oxides: The Role of Oxygen Release

L. Zhou, N. Piekielek, S. Chowdhury, and M. R. Zachariah*

Department of Mechanical Engineering and Department of Chemistry and Biochemistry, University of Maryland, College Park, 20742

Received: February 5, 2010; Revised Manuscript Received: April 16, 2010

In this work, heterogeneous nanocomposite reactions of Al/CuO, Al/Fe₂O₃ and Al/ZnO systems were characterized using a recently developed T-Jump/time-of-flight mass spectrometer. Flash-heating experiments with time-resolved mass spectrometry were performed at heating rates in the range of $\sim 10^5$ K/s. We find that molecular oxygen liberated during reaction is an active ingredient in the reaction. Experiments also conducted for neat Al, CuO, Fe₂O₃, and ZnO powders show that the oxygen are produced by decomposition of oxidizer particles. Mass spectrometric analysis indicates that metal oxide particles behave as an oxygen storage device in the thermite mixture and release oxygen very fast to initiate the reaction. A clear correlation is observed between the capability of oxygen release from oxidizing particles and the overall reactivity of the nanocomposite. The high reactivity of the Al/CuO mixture can be attributed to the strong oxygen release from CuO, while Fe₂O₃ liberates much less oxygen and leads to moderate reactivity, and ZnO's poor oxygen release capability caused the Al/ZnO mixture to be completely not reacting, even though the reaction is overall exothermic. It is likely that the role of the oxygen species is not only as a strong oxidizer but also an energy propagation medium that carries heat to neighboring particles.

Introduction

In recent years, nanocomposites containing a metal fuel and a metal oxide, also known as metastable intermolecular composites (MIC), have attracted great interest compared to their micrometer-sized counterparts.^{1,2} In most formulations, aluminum is used as a fuel because of its high energy density and low cost, and metal oxides such as CuO and Fe₂O₃ are commonly used as oxidizers. Compared with traditional organic energetic materials, these reactions are characterized by higher energy release but slow reaction rates due to mass transfer limits. In nanocomposite MICs, the reactive components are mixed at the nanoscale so that diffusion lengths can be greatly reduced, and the surface area can be increased. As a result nanostructured particles have a much higher reactivity than their corresponding micrometer-sized cousins. Aside from the fast reaction rate, the unique nanostructure of MICs also allows a control over the reactivity by varying parameters such as particle size, morphology and local composition.^{3–5} The general question that is of interest is how do solids react so quickly, and what are the relevant size scaling effects.

Studies of energetic materials are very difficult due to their fast and intense reaction. Measurement of combustion properties such as flame speed, burn rate, or ignition temperatures are typical methods to characterize these reactions.^{1,2,6–11} The reaction mechanism is often studied with traditional thermal analysis techniques such as thermogravimetric analysis (TGA), differential thermal analysis (DTA), or differential scanning calorimetry (DSC). With the help of electron microscopy and X-ray diffraction, reaction products and detailed reaction kinetics at slow heating rates can be revealed.^{12–14} While experimental data obtained from low heating rate conditions can be extrapolated to the high heating regime, it has been shown that heating

rate has an effect on the reaction process.^{1,13–15} Reaction pathways or mechanisms can change drastically from a slow heating process to a fast heating process; therefore, it is preferred to conduct experiments under high heating rates that are more comparable to that of ignition and combustion events. Many experimental techniques have been developed to study thermite reactions under combustion-like conditions.^{2,16–19} In particular, a hot filament heating technique has been widely used in studying reaction kinetics under high heating rates.^{15,20,21} and this approach was also applied for kinetic analysis of nanocomposite reactions.^{13,14}

To capture the processes occurring in fast condensed state reactions we recently developed a temperature-jump/time-of-flight mass spectrometer (T-Jump/TOFMS) whereby condensed state reactions can be initiated from a rapidly heated fine wire containing the reactants placed within the ion-extraction region of a time-of-flight mass spectrometer.²² In this paper, we selected three systems based on their reactivity measured by a constant volume pressure cell, aluminum/copper oxide (Al/CuO), which is known to be highly reactive, aluminum/iron oxide (Al/Fe₂O₃) nanocomposite, which is only moderately reactive, and aluminum/zinc oxide (Al/ZnO), which has very poor reactivity. The characteristic thermochemistry behavior of the oxidizer particles CuO, Fe₂O₃, and ZnO were also investigated. Results suggest the reactivity of thermite mixtures is correlated with the thermal decomposition and oxygen release of oxidizer particles rather than the overall thermochemistry.

Experimental Section

1. Sample Preparation. Nanocomposite samples were prepared by mixing aluminum nanoparticles with oxidizer particles to obtain a stoichiometric mixture. The aluminum used was 50 nm ALEX powder obtained from Argonide Corporation. Copper oxide (CuO) iron oxide (Fe₂O₃), and zinc oxide (ZnO) nanopowders of ~ 100 nm obtained from Sigma-Aldrich. TGA

* To whom correspondence should be addressed. E-mail: mrz@umd.edu. Phone: 301-405-4311. Fax: 301-314-9477.

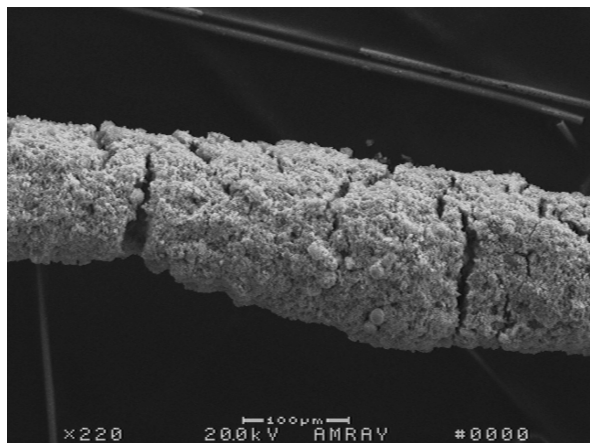


Figure 1. SEM image of T-Jump probe coated with Al/CuO nanocomposite mixture.

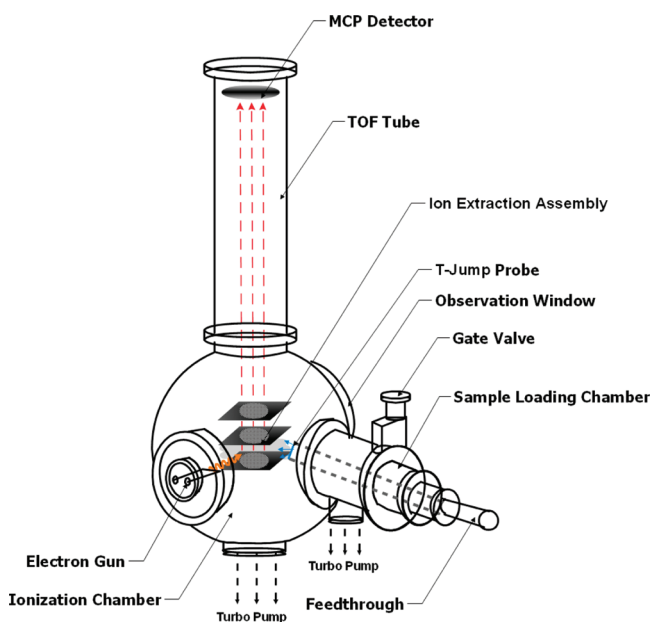


Figure 2. Schematic of the T-Jump/TOFMS.

showed the ALEX powder is 82% aluminum (by mass) with an outer oxide shell and was accounted for in the preparation of stoichiometric samples (equivalence ratio of 1). Samples were mixed in hexane, and the suspensions were sonicated for about 30 min to break the agglomerates and ensure mixing between the fuel and oxidizer. The prepared sample suspensions could then be coated on the T-Jump probe with a dropper. The T-Jump probe is a ~ 10 mm long, $76 \mu\text{m}$ diameter platinum wire that was coated with a thin layer of sample over a ~ 5 mm length. The sample packing density is estimated to be 10–20%. The coating thickness can be estimated from scanning electron micros-

copy (SEM) image shown in Figure 1, which would yield ~ 0.3 mg based on an ideal coating geometry model²³ and assuming a uniform particle size of 50 nm.

2. T-Jump/TOFMS. The experimental apparatus of the T-Jump/TOFMS is shown in Figure 2. It is comprised of a linear TOF chamber, an electron gun for ionization, and the T-Jump probe with an electrical feed-through for rapid sample heating. The essence of the instrument is that the T-Jump probe ($76 \mu\text{m}$ Pt wire) is directly inserted close to the electron ionization (EI) region of the mass spectrometer, and the species from T-Jump excitation are continuously monitored by the TOF mass spectrometer. The electron beam is normally operated at 70 eV and 1 mA, with the background pressure in the TOF chamber at $\sim 10^{-9}$ atm. In each experiment, the T-Jump filament is coated with a thin layer of sample powder which can be heated with an in-house built power source at a rate of up to $\sim 10^6$ K/s. The filament is replaced after each heating event. A detailed description of the operation of T-Jump/TOFMS can be found in a previous paper.²² Briefly, the heating of the T-Jump probe is synchronized with the TOF measurement system. A series of mass spectra as well as the temporal voltage and current of the T-Jump probe during the heating event is recorded by a 500 MHz digital oscilloscope. From the current and voltage trace, a resistivity measurement can be obtained and related to the instantaneous temperature of the filament, which can be mapped against the mass spectra. Time resolved mass spectra combined with temperature information are then used for characterization of nanocomposite thermite reactions.

Recently, we reported the finding of intense ejection of ionized species coincident to or in some cases just before visible reaction.²⁴ The current pulse caused a catastrophic malfunction of the high voltage bias on the ion extraction optics and resulted in a loss of mass spectrum signal. As a result, it was necessary to modify the ion optics configuration to minimize the effect of electric impulse and enable the collection of spectra. In the new configuration, the ion extraction repeller plate and extraction plate are DC biased at ground to avoid collecting electrons/ions generated from the thermite event. The extraction plate is pulsed from ground to -200 V by a high voltage pulser for ion extraction. A liner system is employed within the flight tube and biased to DC -1500 V, together with the acceleration plate, to transport the ion beam to the MCP detector. This configuration successfully prevents loss of spectral signal caused by the highly violent reaction. Figure 3 shows example snapshots taken with a high speed camera during the flash heating for an Al/CuO nanocomposite. The ignition front is first observed at the two ends of the sample coating which propagates toward the center and this ignition behavior is highly reproducible. This is because the thermal coupling between the sample powder and T-Jump wire at the end of the coating pose a smaller heat load and thus reach the ignition temperature first. From the standpoint of our mass spectrometry this has little impact since

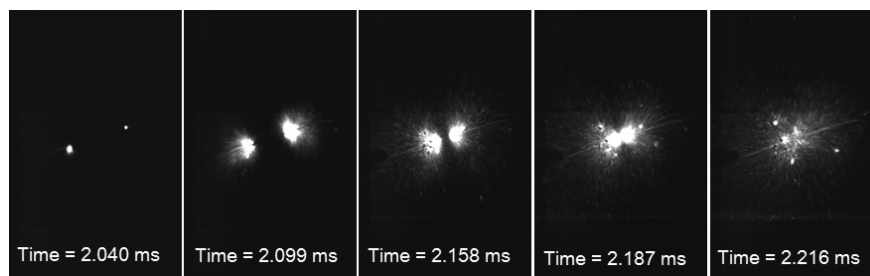


Figure 3. Selected images for a Al/CuO nanocomposite reaction recorded by a high-speed camera.

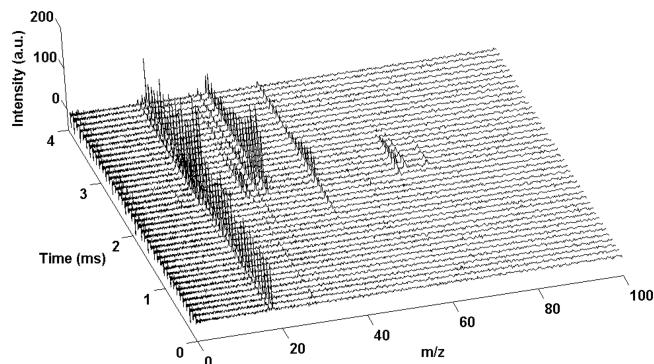


Figure 4. Time-resolved mass spectra obtained from Al/CuO nanocomposite reaction. Sample heating start at $t = 0$.

the propagation time is only $\sim 100 \mu\text{s}$ and thus approximately one mass spectral sampling time. It is also interesting to note that the sample is blown off the wire because of the gas produced from reaction but continues to react due to its intrinsic self-generating energy. In a parallel experiment, the T-Jump technique was coupled with a photomultiplier tube (PMT) setup for the measurement of the optical emission from the nanocomposite thermite reaction. The experiments used the same T-Jump wire except that the experiments were performed at atmospheric pressure. As a useful supplemental experiment, the PMT traces for the nanocomposite reactions were compared with the T-Jump/TOF Mass Spectrometry results.

Results and Discussion

1. Mass Spectrometry Measurements of Nanocomposite Reactions. Nanocomposite mixtures of Al/CuO, Al/Fe₂O₃, and Al/ZnO as well as aluminum, CuO, Al₂O₃, Fe₂O₃, and ZnO nanoparticles were examined under rapid heating conditions. In each heating event, the T-Jump probe was heated to ~ 1700 K with an ~ 3 ms voltage pulse, so that the heating rate is about 5×10^5 K/s. Simultaneously, a sequence of 95 spectra with mass to charge ratio (M/z) up to 400 was recorded with a temporal resolution of $100 \mu\text{s}$ per spectrum. An example mass spectra for rapid heating of a Al/CuO sample are shown in Figure 4.

The first 41 mass spectra out of total 95 spectra are plotted, which corresponds to 0–4 ms of reaction time. The mass spectra in Figure 4 clearly show the progression of the reaction as ion species appear and then decay away. Similar results were obtained for other samples and are shown in Figure 5. Because of limitations of space, we select only one mass spectrum for each measurement, which provides an instantaneous snapshot of a reaction event for a particular stoichiometric mixture. At the start of the heating event, $t = 0$, the spectrum recorded is that of the background in the ion source region, which consists of water (M/z 18) as a primary species and a small amount of N₂ (M/z 28) and O₂ (M/z 32) as shown in Figure 5a. OH⁺ ions ($M/z = 17$) from e-impact fragmentation of water are also observed. As time advances to the ignition point, the thermite reaction is initiated, and new peaks corresponding to reaction products can be observed. Figure 5b is a typical mass spectrum for Al/CuO nanocomposite thermite reaction. New species of O ($M/z = 16$), Al ($M/z = 27$), CO₂ ($M/z = 44$), Cu ($M/z = 63, 65$), and Al₂O ($M/z = 70$) are identified. Similarly, Figure 5c is a mass spectrum obtained from an Al/Fe₂O₃ nanocomposite experiment. New species of Al ($M/z = 27$), H₂CO ($M/z = 30$), CO₂ ($M/z = 44$), Fe ($M/z = 56$), and Al₂O ($M/z = 70$) are identified. No mass-spectral signals are observed that correspond to the hexane solution used to coat the particles, indicating that the sample is free of solvent effects. Similar experiments were also conducted for Al, CuO, Fe₂O₃, and ZnO powders without mixing with their corresponding coreactant and shown in parts d–g of Figure 5, respectively. We also tested Al/ZnO mixture with T-Jump/TOFMS, but the resulting mass spectra show exactly the same pattern as the neat ZnO powders heating (Figure 5g), which implies that the Al/ZnO system is not reacting under our flash-heating conditions.

The mass spectra shown in Figure 5 enable us to identify the thermite reaction products for Al/CuO and Al/Fe₂O₃ systems. We first categorize the observed species into three groups. Group 1: Species of Al, Al₂O, Cu, and Fe are the first category. Group 2: Species of CO, H₂CO, and CO₂ all contain carbon and are probably originated from the same source. Group 3: Oxygen species. Oxygen atom is presumed to be from fragmentation of

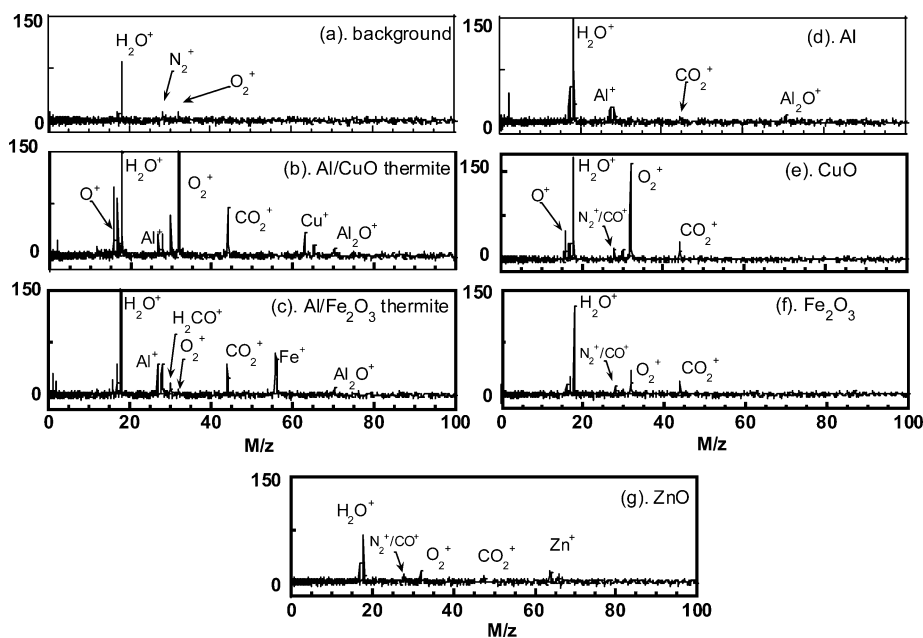


Figure 5. Detailed views of selected mass spectra obtained from T-Jump experiments. (a) Background, (b) Al/CuO mixture, (c) Al/Fe₂O₃ mixture, (d) Al particles, (e) CuO particles, (f) Fe₂O₃ particles, (g) ZnO particles.

the O₂ molecule during electron beam ionization, so O and O₂ form the third category. The species in the first category are compounds from the nanocomposite and are apparently coming from the thermite reaction. However the origin of the second group is ambiguous. To assign the source of CO, H₂CO, and CO₂, we conduct neat Al, CuO, and Fe₂O₃ powders flash-heating experiments (parts d–f of Figure 5, respectively). As we can see species of CO, H₂CO, and CO₂ are mainly observed from heating of CuO and Fe₂O₃ particles. We also notice that the intensity of the water signal increases upon heating indicating that the powders have absorbed water. It is well known that water catalyzes the formation of copper carbonate (CuCO₃) shell on CuO or an iron carbonate (FeCO₃) shell on Fe₂O₃. Upon heating the carbonate shell decomposes to liberate CO, H₂CO, and CO₂ as identified in the spectra. Presumably this carbonate layer is only on the surface of particles, and should be very thin. On the other hand, Al and Al₂O are observed in Figure 5d by simply heating Al powder. The Al₂O species probably originates from the Al₂O₃ shell, while the Al peak suggests that the Al core melts which enables diffusion out from the shell under heating. This has been previously observed by us in slow heating TEM imaging.^{25,26} Notice that only elemental Al is observed in the mass spectra, and no high-order clusters such as Al₂, Al₃, ... are observed; this suggests a diffusive mechanism in our T-Jump ignition experiments instead of an explosive reaction predicted by the “melt-dispersion mechanism”.^{27,28} The species in the third group (O, O₂) are of particular interest as free oxygen could be a key component in the reaction dynamics. As we can see in parts d–f of Figure 5, no oxygen species are observed in heating of Al powder but a significant amount of O₂ is released from heating of CuO and Fe₂O₃ powder, implying that the oxygen observed during the reaction event is from the metal oxide particles. In addition, no Cu or Fe species is observed upon heating of CuO or Fe₂O₃ powder (parts e and f of Figure 5), implying that the Cu or Fe peak observed in the experiments should be a product from the reaction with aluminum.

2. Oxygen Release and Its Relationship to Reactivity. On the basis of the species identified in the time-resolved mass spectra obtained from T-Jump experiments, we are in the position to extract mechanistic information about the reaction phenomena. As we discussed in the previous section, an O₂ peak, in addition to Al, Al₂O, and Cu or Fe, is observed in the mass spectra from Al/CuO or Al/Fe₂O₃ reactions. It is interesting to notice that the mass spectra obtained from the Al/Fe₂O₃ reaction (Figure 5c) shows a weak O₂ peak, but a much higher oxygen peak was clearly observed in Figure 5f from the heating of Fe₂O₃ nanoparticles; this comparison evidently shows that the oxygen species is consumed in the reactions of Al/Fe₂O₃ system. In the case of Al/CuO system, the similar mass spectra comparison is ambiguous since CuO releases abundant oxygen such that both the O₂ signals in parts b and e of Figure 5 are intense. Nevertheless, it is reasonable to believe that oxygen is an active ingredient in the reactions considering the fact that the oxygen is a strong oxidizer and the most mobile species in the system. In fact, if we examine the mass spectra in parts b and c of Figure 5, we can see the signal intensities for species of Al, Al₂O, and Cu/Fe observed from Al/CuO system are quite similar compared to that shown in Al/Fe₂O₃ systems. The only difference between these two systems is the oxygen signal, where Al/CuO system releases more O₂ in contrast to Al/Fe₂O₃ system. This result implies the chemistry of nanocomposite thermite reactions is closely related to the oxygen generation process.

TABLE 1: Pressure Cell Measured Result and Calculated Thermochemical Properties

	Al/CuO	Al/Fe ₂ O ₃	Al/ZnO
measured pressurization rate	~10 psi/ μ sec	~0.01 psi/ μ sec	no combustion
calculated adiabatic temperature	2837 K	3135 K	1822 K
calculated enthalpy of combustion (per mol of Al)	-604.05 kJ/mol	-425.1 kJ/mol	-312.1 kJ/mol

The general combustion behavior was previously evaluated using a constant volume pressure cell,^{4,29} where the reactivity in terms of pressurization rates were measured for these systems and listed in table 1. As we expected, the Al/CuO nanocomposites give a superior pressurization rate of ~10 psi/ μ sec, compared to Al/Fe₂O₃ mixture's ~0.01 psi/ μ sec. In this case the ZnO system did not react, consistent with our T-Jump/TOFMS results. It should be pointed out that the calculated thermochemistry properties listed in Table 1, for the three systems, especially for Al/CuO and Al/Fe₂O₃ systems are not significantly different from each other. The 3 orders of magnitude difference in pressurization rate clearly suggests the Al/CuO system has a much higher reactivity than the Al/Fe₂O₃ mixture. On the other hand, the mass spectrometric measurements demonstrated that metal oxide particles liberate oxygen upon heating, and the oxygen release processes for different oxidizers are distinctively different; therefore the question is how does the characteristic behavior of oxygen generation correlated with the reactivity.

Since the mass spectra were recorded in a time-resolved manner, we plot the O₂ peak intensity obtained from the flash-heating of CuO, Fe₂O₃, and ZnO particles as a function of time and the result is shown in Figure 6. The real-time Pt wire temperature trace is also plotted in Figure 6 to determine the onset decomposition temperatures. Figure 6 shows that the decomposition process of CuO starts at an onset temperature of ~1150 K, and much lower than the ~1450 K observed for Fe₂O₃. Furthermore, the O₂ signal intensity observed during the CuO heating experiment is about 3 times higher than that of the Fe₂O₃, which clearly suggests more oxygen was liberated

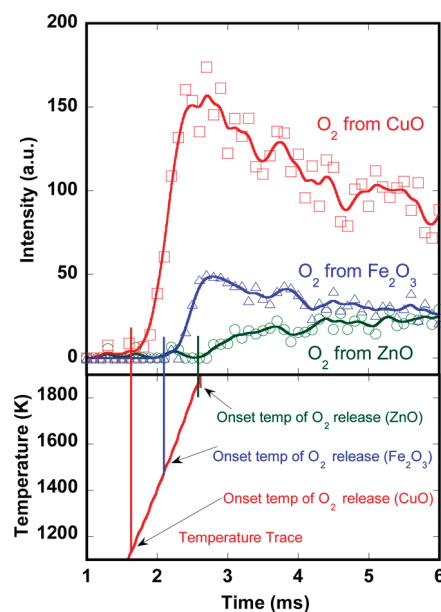


Figure 6. Temporal profile of oxygen peak intensity from heating of CuO, Fe₂O₃, and ZnO nanoparticles.

from flash heating of CuO. The fact that CuO is able to generate an abundance of oxygen gas relatively easily is thus also likely the reason for the high reactivity of the Al/CuO relative to Al/Fe₂O₃, despite the fact that the overall thermochemistry would argue the iron system as the more energy dense (Al/CuO 2837 K vs Al/Fe₂O₃ 3135 K at atmospheric pressure, from NASA Chemical Equilibrium with Applications (CEA) calculation). For ZnO, it is clear that ZnO releases the least amount of total oxygen among all three oxidizers and releases it at a higher temperature and at a slower rate. But perhaps a more interesting detail is that the onset of ZnO decomposition is at ~1900 K, which is higher than the calculated adiabatic flame temperature of ~1822 K for the Al/ZnO system. In other words, even if we heat an initial layer of ZnO to its decomposition temperature so that we have a reacting Al/ZnO system, the energy release would not be sufficient to sustain the reaction and allow it to propagate. So even though the reaction is overall exothermic, the intermediate step of O₂ release is sufficiently uphill so as to prevent reaction propagation. This illustrates that the overall thermochemistry only provides a partial picture of reactivity. The results obtained in the wire studies are consistent with the pressure cell bulk measurements. The results we believe clearly demonstrate the key importance of O₂ release kinetics from the metal oxide in this class of reactions and that the overall thermochemistry is not a good indicator of reactivity.

To further illustrate the relevance of metal oxide decomposition we present thermochemical calculations for CuO and Fe₂O₃ decomposition under vacuum condition (10⁻⁹ atm). The mole fractions of gaseous products are calculated at selected temperatures in the range from room temperature to 3000 K, and the results are shown in parts a and b of Figure 7 for CuO and Fe₂O₃ respectively. The CuO remains stable until ~750 K, and starts to decompose to form Cu₂O and O₂ (4CuO → 2Cu₂O + O₂). As the temperature increases to above ~1050 K, the reduced zerovalent metal is formed. On the other hand, equilibrium calculation shows that Fe₂O₃ is much more stable than CuO. The decomposition of Fe₂O₃ to form Fe₃O₄ and O₂ (6Fe₂O₃ → 4Fe₃O₄ + O₂) requires a higher temperature of ~1100 K and also releases less O₂ than CuO and will fully decompose as the temperature increases to above 1400 K. These calculation results are qualitatively consistent with the experimental observation shown in Figure 6. The equilibrium calculations show that CuO and Fe₂O₃ have distinctive decomposition temperatures and imply that there should be a correlation between the decomposition temperature and the reaction ignition temperature. The ignition temperatures of Al/CuO and Al/Fe₂O₃ nanocomposite mixtures can be determined from our T-Jump/TOFMS, and the range of the ignition temperatures we observed from those experiments are shown in parts a and b of Figure 7. As we expected, the ignition temperatures for Al/CuO are as low as ~850 K, significantly lower than the ~1100 K observed for Al/Fe₂O₃ system. It is obvious that the range of ignition temperatures matches the thermal equilibrium calculation predicted temperature range for oxidizer decomposition. Next we turn our attention to the general temporal behavior. The normalized peak intensities of the major peaks as a function of time are shown for an Al/CuO and Al/Fe₂O₃ in parts a and b of Figure 8, respectively. For both metal oxides we see that group 2 species CO (*M/z* = 28) and CO₂ (*M/z* = 44) appear before species from other groups, implying that the carbonate layer is first removed by thermal decomposition before the exothermic reaction event commences. As time advanced to ~1.8 ms in Figure 8a (Al/CuO mixture) or ~2.5 ms in Figure 8b (Al/Fe₂O₃ mixture), species of Al, Al₂O, Cu, and O₂ (for Al/CuO) or Al, Al₂O, and Fe (for Al/Fe₂O₃) begin

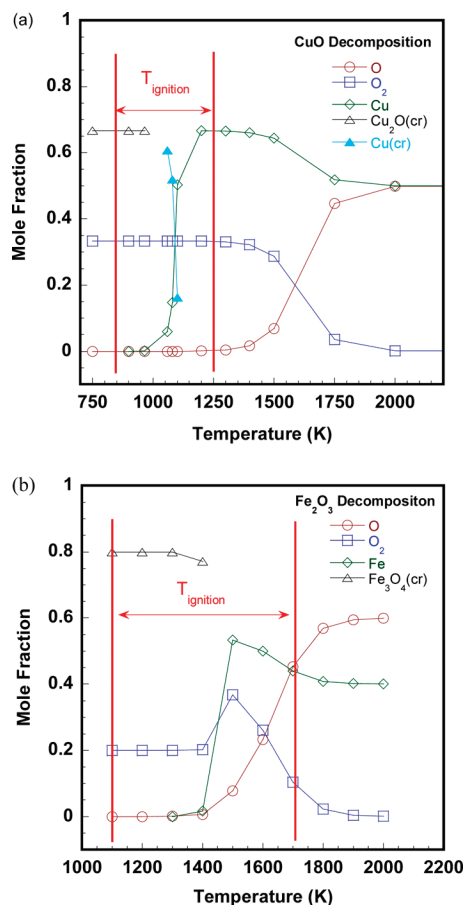


Figure 7. Results of thermal equilibrium calculation using CEA code for (a) CuO decomposition and (b) Fe₂O₃ decomposition. T_{ignition} is ignition temperature of nanocomposite reactions measured from T-Jump/TOFMS.

to appear, and ignition is considered to occur. As discussed early, the significant difference between the Al/CuO system and the Al/Fe₂O₃ system is the formation of oxygen species. The mass spectra of the Al/CuO reaction shows a strong O₂ peak, with a temporal profile (Figure 8a) following the same trend as the other species, implying that oxygen is a reactive species and involved in the thermite reaction. On the basis of these mass spectrometric observations, we can conclude that the reaction of the nanocomposite occurs in the following steps: (1) decomposition of CuCO₃ or FeCO₃ shell, (2) CuO or Fe₂O₃ decomposition (4CuO → 2Cu₂O + O₂ or 6Fe₂O₃ → 4Fe₃O₄ + O₂) and melting, and release of the Al core, (3) Al reacting with oxygen, (4) and once there is enough oxygen released the reaction with Al, becomes self-sustained, and the thermite reaction is then fully ignited and further reaction involves Al fuel reacting with oxidizers including oxygen gas and metal oxides. Here we would also like to point out that although the reaction steps are explained with an emphasis on the role of oxygen, the process of how Al fuel becomes involved has a great influence on the overall reaction. The fact that the temporal profile of the Al signal shares a similar trend with O₂, suggests both fuel and oxidizer are required to be in contact with each other for the initiation of the reaction. Since the Al fuel is a core-shell structured particle with aluminum core and outside aluminum oxide shell, the transport mechanism on how the active Al releases becomes very important in understanding the thermite reaction behavior and is the subject of considerable research effort.^{27,28,30}

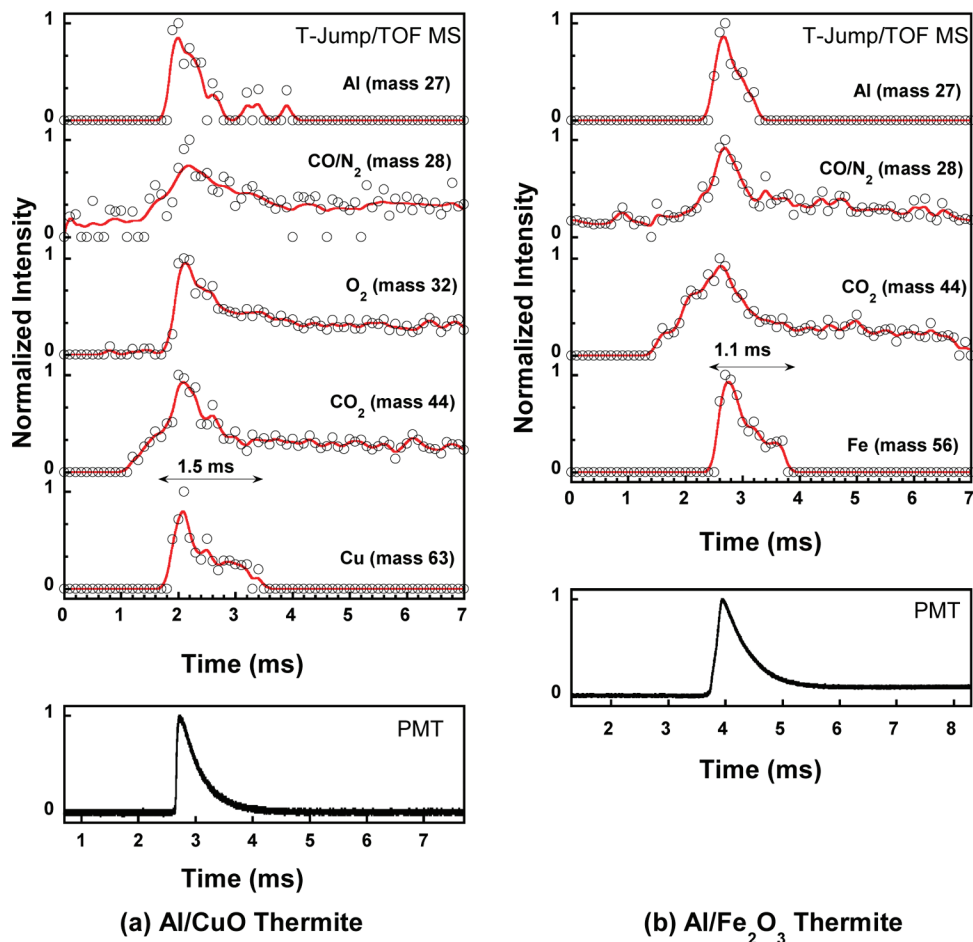


Figure 8. Normalized peak intensities as function of reaction time for reaction species observed in (a) Al/CuO and (b) Al/Fe₂O₃ reactions; the bottom plots are optical signal measured from separated experiments.

As a complement to the T-Jump/TOFMS experiments, optical emission from the nanocomposite reaction was also measured at atmospheric pressure. The optical emissions for these reactions, after background corrections, are shown at the bottom of Figure 8 (a) for Al/CuO and (b) for Al/Fe₂O₃. The rapid rise in the optical signal indicates the onset of ignition. There is a slight difference in the time to ignition as observed through the PMT due to experimental run-to-run uncertainty. Hence, the PMT signals have been presented with a small time offset to compare with the MS signal. The widths of the PMT trace are ~1.5 ms and ~1.1 ms for Al/CuO and Al/Fe₂O₃, respectively, and agree with the MS signal very well. These also indicate that the combustion time as measured mass spectrometrically and optically are consistent and provide a measure of the reaction time. Since the optical measurements were conducted in air, while the MS measurement was in vacuum, this result suggests the presence of oxygen in air has little effect, compared to the oxygen released from the oxidizer particles. If one assumes a mass transfer limited mechanism, and compares the amount of oxygen liberated from decomposition of the oxide with the amount of oxygen in air, we can estimate the relative importance of these two sources of oxygen. Since particles are loosely packed in our experiments, we consider a control volume, where an aluminum particle mixed with a CuO particle to form a stoichiometric mixture (based on reaction $2\text{Al} + 3\text{CuO} \rightarrow \text{Al}_2\text{O}_3 + 3\text{Cu}$), and then the oxygen concentration in this unit cell due to CuO decomposition is given by

$$C_{\text{O}_2} = \frac{\eta m_{\text{O}_2}}{V} = \frac{3\eta M_{\text{O}_2}}{8VM_{\text{Al}}} m_{\text{Al}} \quad (1)$$

where η is particle packing density, V is the volume of the particles, M_{O_2} and M_{Al} are molecular weight of oxygen gas and aluminum, respectively, and m_{Al} is the mass of the aluminum particle. For 50-nm aluminum particles and 15% packing, the oxygen concentration is estimated to be ~55 kg/m³. On the other hand, the oxygen concentration in the control volume due to ambient air is 0.27 kg/m³ at room temperature and only 0.06 kg/m³ at 1300 K and thus about 3 orders of magnitude less than the oxygen liberated from the CuO particles. This calculation suggests the metal oxide particles behave as an oxygen storage device and can release oxygen very fast to initiate the reaction. This may also explain why aluminum particles burn much faster if mixed with metal oxide than combustion in air. Additional optical experiments carried out in an argon environment, are essentially indistinguishable from that in air, corroborating the above analysis and conclusion.

Conclusions

In this work, nanocomposite reactions of Al/CuO, Al/Fe₂O₃, and Al/ZnO systems are probed with a newly developed time-resolved T-Jump/TOFMS. Time-resolved mass spectra were obtained for the reaction of Al/CuO and Al/Fe₂O₃ nanocomposites, and the Al/ZnO system shows no reactivity. Species of Al, Al₂O, and Cu/Fe were identified from mass spectra. Analysis suggests the initial steps of the thermite reaction are the

decomposition of the oxidizer particles to form oxygen as well as Al diffusion through the Al_2O_3 shell. The experimental data support the theory that the formation of oxygen from oxidizer particles should be an important factor in the reaction of nanocomposite mixtures. We find the reactivity of nanocomposite MICs is strongly associated with the oxidizer's capability to release oxygen rapidly, rather than the overall thermochemistry (exothermicity).

Acknowledgment. This work was supported by the Defense Threat Reduction Agency, the Army Research Office, and the University of Maryland Center for Energetic Concepts Development.

References and Notes

- (1) Pantoya, M. L.; Granier, J. J. The effect of slow heating rates on the reaction mechanisms of nano and micron composite thermite reactions. *J. Therm. Anal. Combust.* **2006**, *85* (1), 37–43.
- (2) Granier, J. J.; Pantoya, M. L. Laser ignition of nanocomposite thermites. *Combust. Flame* **2004**, *138* (4), 373–383.
- (3) Umbrajkar, S. M.; Seshadri, S.; Schoenitz, M.; Hoffmann, V. K.; Dreizin, E. L. Aluminum-rich Al-MoO₃ nanocomposite powders prepared by arrested reactive milling. *J. Propulsion Power* **2008**, *24* (2), 192–198.
- (4) Sullivan, K.; Young, G.; Zachariah, M. R. Enhanced Reactivity of Nano-B/Al/CuO MICs. *Combust. Flame* **2009**, *156*, 302.
- (5) Prakash, A.; McCormick, A. V.; Zachariah, M. R. Tuning the reactivity of energetic nanoparticles by creation of a core-shell nanostructure. *Nano Lett.* **2005**, *5* (7), 1357–1360.
- (6) Young, G.; Sullivan, K.; Zachariah, M. R. Combustion Characteristics of Boron Nanoparticles. *Combust. Flame* **2009**, *156*, 332.
- (7) Son, S. F.; Asay, B. W.; Foley, T. J.; Yetter, R. A.; Wu, M. H.; Risha, G. A. Combustion of nanoscale Al/MoO₃ thermite in microchannels. *J. Propulsion Power* **2007**, *23* (4), 715–721.
- (8) Sanders, V. E.; Asay, B. W.; Foley, T. J.; Tappan, B. C.; Pacheco, A. N.; Son, S. F. Reaction propagation of four nanoscale energetic composites (Al/MoO₃, Al/WO₃, Al/CuO, and Bi₂O₃). *J. Propulsion Power* **2007**, *23* (4), 707–714.
- (9) Shoshin, Y. L.; Trunov, M. A.; Zhu, X.; Schoenitz, M.; Dreizin, E. L. Ignition of aluminum-rich Al-Ti mechanical alloys in air. *Combust. Flame* **2006**, *144* (4), 688–697.
- (10) Trunov, M. A.; Schoenitz, M.; Dreizin, E. L. Ignition of aluminum powders under different experimental conditions. *Propellants Explosives Pyrotechnics* **2005**, *30* (1), 36–43.
- (11) Plantier, K. B.; Pantoya, M. L.; Gash, A. E. Combustion wave speeds of nanocomposite Al/Fe₂O₃: the effects of Fe₂O₃ particle synthesis technique. *Combust. Flame* **2005**, *140* (4), 299–309.
- (12) Mei, J.; Halldearn, R. D.; Xiao, P. Mechanisms of the aluminium-iron oxide thermite reaction. *Scripta Mater.* **1999**, *41* (5), 541–548.
- (13) Schoenitz, M.; Umbrajkar, S.; Dreizin, E. L. Kinetic analysis of thermite reactions in Al-MoO₃ nanocomposites. *J. Propulsion Power* **2007**, *23* (4), 683–687.
- (14) Umbrajkar, S. M.; Schoenitz, M.; Dreizin, E. L. Exothermic reactions in Al-CuO nanocomposites. *Thermochim. Acta* **2006**, *451* (1–2), 34–43.
- (15) Brill, T. B.; Beckstead, M. C.; Flanagan, J. E.; Lin, M. C.; Litzinger, T. A.; Waesche, R. H. W.; Wight, C. A. Chemical speciation and dynamics in the surface combustion zone of energetic materials. *J. Propulsion Power* **2002**, *18* (4), 824–834.
- (16) Henric, O.; Nils, R. Laser ignition of pyrotechnic mixtures: Ignition mechanisms. *J. Appl. Phys.* **1993**, *73* (4), 1993–2003.
- (17) Yang, Y.; Sun, Z.; Wang, S.; Dlott, D. D. Fast Spectroscopy of Laser-Initiated Nanoenergetic Materials. *J. Phys. Chem. B* **2003**, *107* (19), 4485–4493.
- (18) Trenkle, J. C.; Koerner, L. J.; Tate, M. W.; Gruner, S. M.; Weihs, T. P.; Hufnagel, T. C. Phase transformations during rapid heating of Al/Ni multilayer foils. *Appl. Phys. Lett.* **2008**, *93* (8), xxx.
- (19) Moore, D. S.; Son, S. E.; Asay, B. W. Time-resolved spectral emission of deflagrating nano-Al and nano-MoO₃ metastable interstitial composites. *Propellants Explosives Pyrotechnics* **2004**, *29* (2), 106–111.
- (20) Brill, T. B.; Arisawa, H.; Brush, P. J.; Gongwer, P. E.; Williams, G. K. Surface Chemistry of Burning Explosives and Propellants. *J. Phys. Chem.* **1995**, *99* (5), 1384–1392.
- (21) Brill, T. B.; Brush, P. J.; James, K. J.; Shepherd, J. E.; Pfeiffer, K. J. T-Jump/FT-IR Spectroscopy: A New Entry into the Rapid, Isothermal Pyrolysis Chemistry of Solids and Liquids. *Appl. Spectrosc.* **1992**, *46*, 900–911.
- (22) Zhou, L.; Piekielek, N.; Chowdhury, S.; Zachariah, M. R. T-Jump/Time-of-Flight Mass Spectrometry for Time Resolved Analysis of Energetic Materials. *Rapid Commun. Mass Spectrom.* **2009**, *23* (1), 194–202.
- (23) Ward, T. S.; Trunov, M. A.; Schoenitz, M.; Dreizin, E. L. Experimental methodology and heat transfer model for identification of ignition kinetics of powdered fuels. *Int. J. Heat Mass Transf.* **2006**, *49* (25–26), 4943–4954.
- (24) Zhou, L.; Piekielek, N.; Chowdhury, S.; Lee, D.; Zachariah, M. R. Transient ion ejection during nanocomposite thermite reactions. *J. Appl. Phys.* **2009**, *106*, 083306.
- (25) Rai, A.; Park, K.; Zhou, L.; Zachariah, M. R. Understanding the mechanism of aluminium nanoparticle oxidation. *Combust. Theor. Model.* **2006**, *10* (5), 843–859.
- (26) Rai, A.; Lee, D.; Park, K.; Zachariah, M. R. Importance of Phase Change of Aluminum in Oxidation of Aluminum Nanoparticles. *J. Phys. Chem. B* **2004**, *108* (39), 14793–14795.
- (27) Chowdhury, S.; Sullivan, K.; Piekielek, N.; Zhou, L.; Zachariah, M. R. Diffusive vs Explosive Reaction at the Nanoscale. *J. Phys. Chem. C* **2010**, *114*, 9191.
- (28) Levitas, V. I.; Asay, B. W.; Son, S. F.; Pantoya, M. Melt dispersion mechanism for fast reaction of nanothermites. *Appl. Phys. Lett.* **2006**, *89* (7), 071909.
- (29) Sullivan, K.; Zachariah, M. R. Simultaneous Pressure and Optical Measurements of Nanoaluminum-Based Thermites: An Investigation of the Reaction Mechanism. *J. Propulsion Power* **2010**, *26*, 467.
- (30) Henz, B.; Hawa, T.; Zachariah, M. R. On the Role of Built-in Electric Fields on the Ignition of Oxide Coated NanoAluminum: Ion mobility versus Fickian Diffusion. *J. Appl. Phys.* **2010**, *107*, 024901.